Biological response to the 1997–98 and 2009–10 El Niño events in the equatorial Pacific Ocean

Michelle M. Gierach,[1] Tong Lee,[1] Daniela Turk,[2,3] and Michael J. McPhaden[4]

Received 24 January 2012; revised 11 April 2012; accepted 17 April 2012; published 16 May 2012.

[1] Changes in the physical environment associated with eastern Pacific (EP)-El Niño and central Pacific (CP)-El Niño events affect the biological response in the equatorial Pacific Ocean differently. However, such responses have not been adequately investigated, especially in terms of the relevant physical processes. This paper addresses the mechanistic differences in the biological response of the equatorial Pacific Ocean during the strongest CP- and EP-El Niño to date (i.e., 1997–98 EP-El Niño and 2009–10 CP-El Niño) using satellite data and water mass pathway analysis based on an ocean reanalysis product. The 1997–98 EP-El Niño was associated with a larger reduction of chlorophyll-a (chl-a) in the eastern equatorial Pacific (EEP) and the 2009–10 CP-El Niño was associated with a larger reduction of chl-a in the central equatorial Pacific (CEP). These biological responses were dependent on the strength and extent of westerly wind anomalies and their impact on horizontal and vertical processes. Horizontal advection was the primary contributor to differences in chl-a between the two El Niño events in the CEP, whereas vertical advection and mixing were the dominant processes in the EEP. **Citation:** Gierach, M. M., T. Lee, D. Turk, and M. J. McPhaden (2012), Biological response to the 1997–98 and 2009–10 El Niño events in the equatorial Pacific Ocean, *Geophys. Res. Lett.*, *39*, L10602, doi:10.1029/2012GL051103.

1. Introduction

[2] El Niño-Southern Oscillation (ENSO) affects global atmospheric and oceanic conditions on interannual timescales that in turn alter biological production and ecosystem dynamics in many regions, most notably the equatorial Pacific Ocean [*Chavez et al.*, 1999; *McPhaden et al.*, 2006]. Since the 1990s, there have been frequent occurrences of a new type of El Niño with maximum warming in the central equatorial Pacific (CEP) otherwise known as the central Pacific (CP)-El Niño, warm-pool El Niño, dateline El Niño, or El Niño Modoki [*Latif et al.*, 1997; *Larkin and Harrison*, 2005; *Yu and Kao*, 2007; *Ashok et al.*, 2007; *Kao and Yu*, 2009; *Kug et al.*, 2009; *Yu and Kim*, 2010]. This is in contrast to the classic eastern Pacific (EP)-El Niño that has maximum warming in the eastern equatorial Pacific (EEP). The two types of El Niño (CP- and EP-El Niño) have different teleconnections and climatic impacts [e.g., *Weng et al.*, 2009; *Kim et al.*, 2009; *Ashok and Yamagata*, 2009]. The amplitude of El Niño in the CEP has increased significantly over the last three decades, with the 2009–10 event being the strongest CP-El Niño observed to date [*Lee and McPhaden*, 2010].

[3] Previous studies in the tropical Pacific concerning ENSO-induced biological responses have primarily focused on the classic EP-El Niño [*Barber and Chavez*, 1983; *Fiedler et al.*, 1992; *Chavez et al.*, 1998, 1999; *Strutton and Chavez*, 2000; *Turk et al.*, 2001]. These studies documented reduced chlorophyll-a (chl-a) in the EEP and CEP and increased chl-a in the western equatorial Pacific (WEP) associated with changes in thermocline and nutricline depths; these changes were due to westerly wind anomalies that weaken or possibly reverse the trade winds. Recent studies by *Turk et al.* [2011] and *Radenac et al.* [2012] described the biological response in the equatorial Pacific associated with CP-El Niño events as observed from remote sensing observations. *Turk et al.* [2011] and *Radenac et al.* [2012] showed that lower chl-a occurred in the CEP during CP-El Niño as compared to what is observed during EP-El Niño. Neither study provided quantitative assessment about the roles of various physical mechanisms responsible for these differences in chl-a, especially vertical advection and mixing that are difficult to be resolved by observations directly. Despite these previous efforts, significant knowledge gaps exist in our understanding of the biological response of the equatorial Pacific Ocean to different types of El Niño. Specifically, the relative contributions of horizontal and vertical processes on primary production have not been adequately studied.

[4] The purpose of this paper is twofold: 1) to illustrate spatial differences in the biological response in the equatorial Pacific Ocean (5°S–5°N) to the strongest CP- and EP-El Niño events during the Sea-viewing Wide Field-of-view Sensor (SeaWiFS) satellite period (i.e., 1997–2010) and 2) to explain the mechanisms behind these biological differences through examination of variability in the physical environment and relative contributions of horizontal and vertical processes. Since 1990, there have been 3 EP- and 4 CP-El Niño events according to NOAA's definition [e.g., *McPhaden et al.*, 2011]. Of these, the 2009–10 CP- and 1997–98 EP-El Niño were the strongest El Niño events in the SeaWiFS satellite era and therefore are the focus of this study.

2. Data and Methods

[5] Various satellite products were utilized to analyze the biological and physical differences between the 1997–98 EP- and 2009–10 CP-El Niño events. Products included

[1]Jet Propulsion Laboratory, California Institute of Technology, Pasadena, California, USA.
[2]Department of Oceanography, Dalhousie University, Halifax, Nova Scotia, Canada.
[3]Lamont-Doherty Earth Observatory, Earth Institute at Columbia University, Palisades, New York, USA.
[4]Pacific Marine Environmental Laboratory, NOAA, Seattle, Washington, USA.

Corresponding author: M. M. Gierach, Jet Propulsion Laboratory, California Institute of Technology, 4800 Oak Grove Dr., M/S 300-323, Pasadena, CA 91109, USA. (michelle.gierach@jpl.nasa.gov)

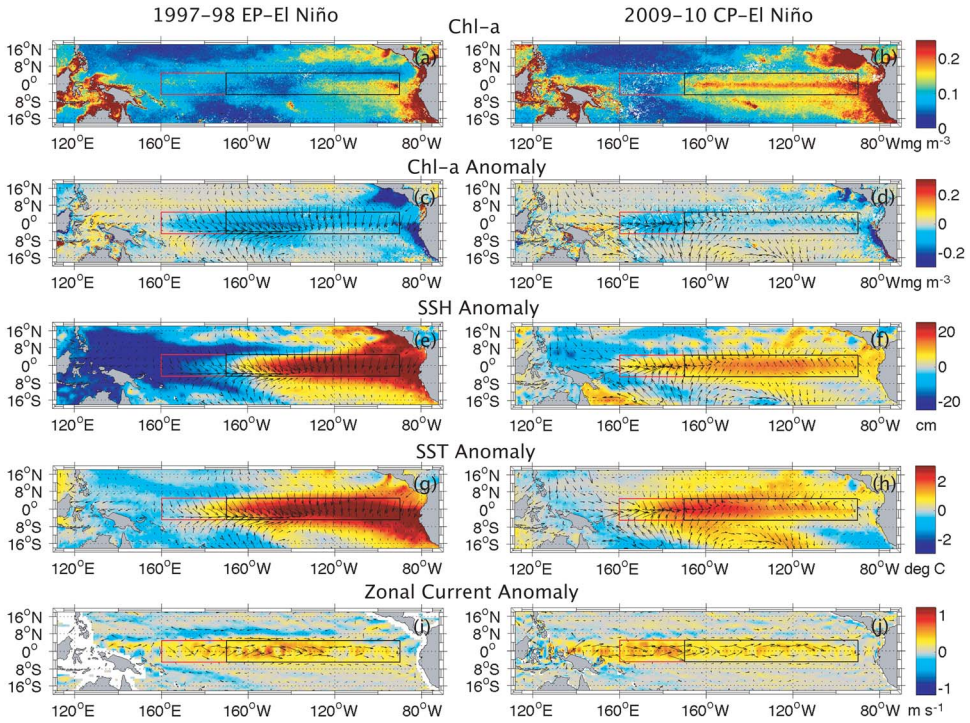

Figure 1. (a, b) November-December-January (NDJ) averaged SeaWiFS chl-a. NDJ averaged anomalies of (c, d) SeaWiFS chl-a, (e, f) AVISO SSH, (g, h) OISST, and (i, j) OSCAR zonal ocean surface currents for the 1997–98 EP-El Niño and 2009–10 CP-El Niño. CCMP wind vector anomalies are overlaid in Figures 1c–1h and ocean surface current vector anomalies in Figures 1i and 1j. The black and red boxes denote the EEP (5°S–5°N, 170°W–90°W) and CEP (5°S–5°N, 160°E–170°W) regions.

9 km SeaWiFS chl-a from Ocean Biology Processing Group (http://oceancolor.gsfc.nasa.gov/), AVISO sea surface height (SSH) on 1/3° Mercator grids (http://www.aviso.oceanobs.com/), 1/4° Group for High Resolution Sea Surface Temperature (GHRSST) AVHRR-based Optimal Interpolation Sea Surface Temperature (OISST) [*Reynolds et al.*, 2007], 1/4° Cross-Calibrated Multi-Platform (CCMP) ocean surface winds [*Atlas et al.*, 2011], and 1/3° OSCAR (Ocean Surface Current Analysis Real-time) ocean surface currents [*Bonjean and Lagerloef*, 2002]. OISST, CCMP, and OSCAR products were obtained from the Physical Oceanography Distributed Active Archive Center (PO.DAAC; http:/podaac.jpl.nasa.gov/) at the NASA Jet Propulsion Laboratory. All satellite products, with the exception of OISST and OSCAR, had monthly temporal resolution. Monthly mean OISST and OSCAR data were obtained by averaging the 5-day ocean surface current and daily SST products. For each satellite product, monthly anomalies were computed as the difference between the individual monthly means and the mean monthly climatology. For consistency among data products, monthly climatologies corresponded to the length of the SeaWiFS data (i.e., 1997–2010).

[6] Tropical oceans are in general nutrient-limited rather than light-limited. Therefore, changes in the physical state associated with El Niño affect biological production by altering the nutrient supply. Here we apply an adjoint passive tracer method, as employed by *Fukumori et al.* [2004] and *Wang et al.* [2004], to characterize the difference in origin of source waters (thus nutrient supply) for different parts of the equatorial Pacific Ocean. The method tracks the origin and pathway of source waters for a particular region and date backwards in time using an advective-diffusive tracer equation of which velocity fields and mixing tensors are derived from estimates of a data assimilation effort as part of the Estimating the Circulation and Climate of the Ocean (ECCO) project. The evolution of passive tracers can quantify the origin of water masses by reflecting advection and mixing processes, which cannot be completely resolved by observations directly. A major difference between this method and the more conventional backward particle trajectory analysis is that the current method includes the effect of mixing. Detailed description of the underlying model, data assimilation procedure, and the adjoint passive tracer method can be found in *Lee et al.* [2002], *Kim et al.* [2007], and *Fukumori et al.* [2004].

[7] For this study, adjoint passive tracer simulations were used to differentiate the relative contribution of horizontal and vertical processes to the biological response observed during the 1997–98 EP- and 2009–10 CP-El Niño (i.e., the origin and pathway of nutrients). Passive tracers were initialized with a unit concentration in the upper 50 m (approximate depth of the average mixed layer) within the EEP (5°S–5°N, 170°W–90°W) and CEP (5°S–5°N, 160°E–170°W). These bounding regions represent areas of considerable chl-a reduction (section 3, Figures 1a–1d and 2b). Initializations for these regions were performed at the end of December 1997 and December 2009 (the month of peak El Niño amplitude identified from SST anomalies). Sensitivity of adjoint tracer distributions to the choice of depth over which the initial tracer was released (e.g., 0–30 m instead of 0–50 m) and the start month (e.g., November instead of December) were examined and results were robust.

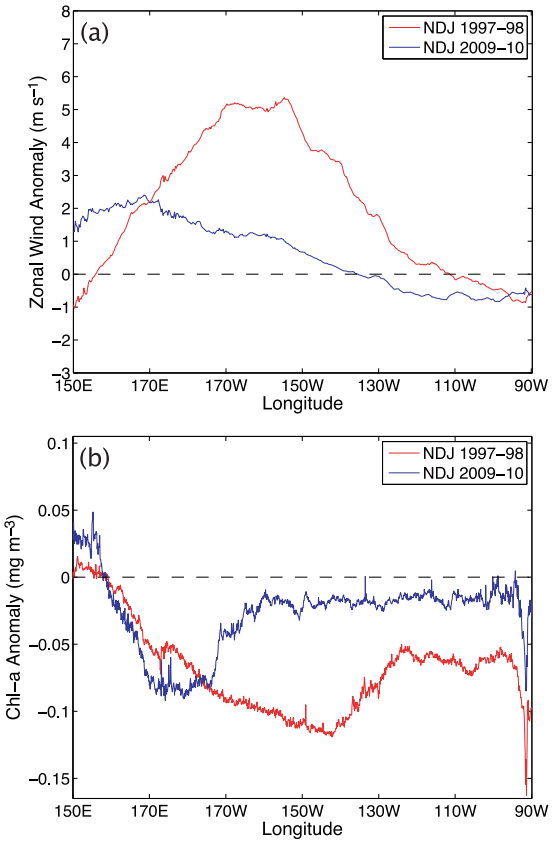

Figure 2. NDJ 5°S–5°N averaged (a) CCMP zonal wind anomaly and (b) SeaWiFS chl-a anomaly in the Pacific during the 1997–98 EP-El Niño (red line) and 2009–10 CP-El Niño (blue line). In Figure 2a positive values indicate westerly wind anomalies (i.e., winds from the west) and negative values easterly wind anomalies (i.e., winds from the east).

For each of these cases, the tracer concentrations in the EEP and CEP were integrated backwards in time for one year (January 1) to determine water mass origin. For this study, we focus on October tracer concentrations as a diagnostic since the physical environment from October to December was representative of mature El Niño conditions. Adjoint tracer distributions were examined for months prior to October and similar conclusions were found. Monthly 20°C isotherm depth data (5°S–5°N average) for October 1997 and October 2009 were also acquired from measurements made by the Tropical Atmosphere Ocean (TAO) buoy array provided by the NOAA Pacific Marine Environmental Laboratory (http://www.pmel.noaa.gov/tao/) as a proxy for the thermocline/nutricline.

3. Results

[8] Satellite observations of November-December-January (NDJ) averaged atmospheric and oceanic conditions during the mature phase of the 1997–98 EP- and 2009–10 CP-El Niño are shown in Figure 1. Consistent with past studies [*Barber and Chavez*, 1983; *Fiedler et al.*, 1992; *Chavez et al.*, 1998, 1999; *Strutton and Chavez*, 2000; *Turk et al.*, 2001, 2011; *Radenac et al.*, 2012], reduced chl-a occurred in the EEP (5°S–5°N, 170°W–90°W) and CEP (5°S–5°N, 160°E–170°W) during the 1997–98 EP- and 2009–10 CP-El Niño (Figures 1a–1d and 2b). However, the magnitude and location of these anomalies differed between events. Within the EEP, chl-a was substantially reduced during the 1997–98 EP-El Niño and was less reduced with patchy increases during the 2009–10 CP-El Niño (Figures 1a–1d and 2b). In contrast, within the CEP there was a notable reduction in chl-a during the 2009–10 CP-El Niño and less of a reduction in chl-a during the 1997–98 EP-El Niño. Such results indicated that the 1997–98 EP-El Niño had a larger impact on the EEP and the 2009–10 CP-El Niño a larger impact on the CEP. This is consistent with *Turk et al.* [2011] and *Radenac et al.* [2012] that noted lower chl-a in the CEP during CP-El Niño.

[9] Biological responses in the CEP and EEP to the 1997–98 EP- and 2009–10 CP-El Niño were dependent on the strength and extent of westerly wind anomalies and their impact on the physical environment (Figures 1 and 2). A considerable reduction in chl-a occurred within the EEP during the 1997–98 EP-El Niño in association with strong westerly wind anomalies that weakened the easterly trade winds (Figures 1a, 1c, 2a, and 2b). Such forcing elevated sea level (implying a depression of the thermocline and nutricline), drove anomalous eastward surface currents, and increased SST in the EEP (Figures 1e, 1g, and 1i). Areas of low chl-a coincided with higher SST and SSH. Smaller increases in SST and SSH were observed in the EEP for the 2009–10 CP-El Niño consistent with weak westerly wind anomalies (Figures 1f, 1h, and 2a). Such physical differences between events implied that upwelling was weakened more substantially in the EEP during the 1997–98 EP- than the 2009–10 CP-El Niño, causing a reduction in the nutrient supply and lower chl-a. In the CEP (e.g., near the dateline) there was stronger eastward advection of warm-pool waters during the 2009–10 event than the 1997–98 event (Figures 1i and 1j). This suggests that the 2009–10 CP-El Niño was associated with a larger intrusion of nutrient-poor warm-pool waters than the 1997–98 EP-El Niño, causing a greater reduction in chl-a in the CEP during the 2009–10 event (Figures 1b, 1d, and 2b). Note that characteristics observed and inferences made during the NDJ period in the CEP region are associated with water mass advection prior to the NDJ period (e.g., August-September-October). Adjoint tracer simulations were used to further illustrate these mechanisms, especially to examine the relative contribution of vertical and horizontal processes to the biological response.

[10] Adjoint tracers were initialized with a unit concentration in the upper 50 m of the EEP and CEP regions for December 1997 and December 2009 and then integrated backwards in time (section 2). Figures 3a and 3b show the longitude-depth distribution of adjoint tracer values integrated from 5°S to 5°N in the EEP for October 1997 and October 2009 overlaid with the depth of the 20°C isotherm (a proxy for the nutricline/thermocline). Tracer distribution values were normalized by the maximum initial tracer concentration (i.e., December 1997 and December 2009) integrated over the same latitudinal bands. A high value indicates greater contribution of the October water mass (nutrient) to the December water mass (nutrient) in the upper 50 m of the EEP. The opposite is true for a low value. In the extreme cases, a value of 1 (0) means all (none) of the October water mass makes its way to the upper 50 m of the EEP by December. Hereafter, these tracer concentrations are referred

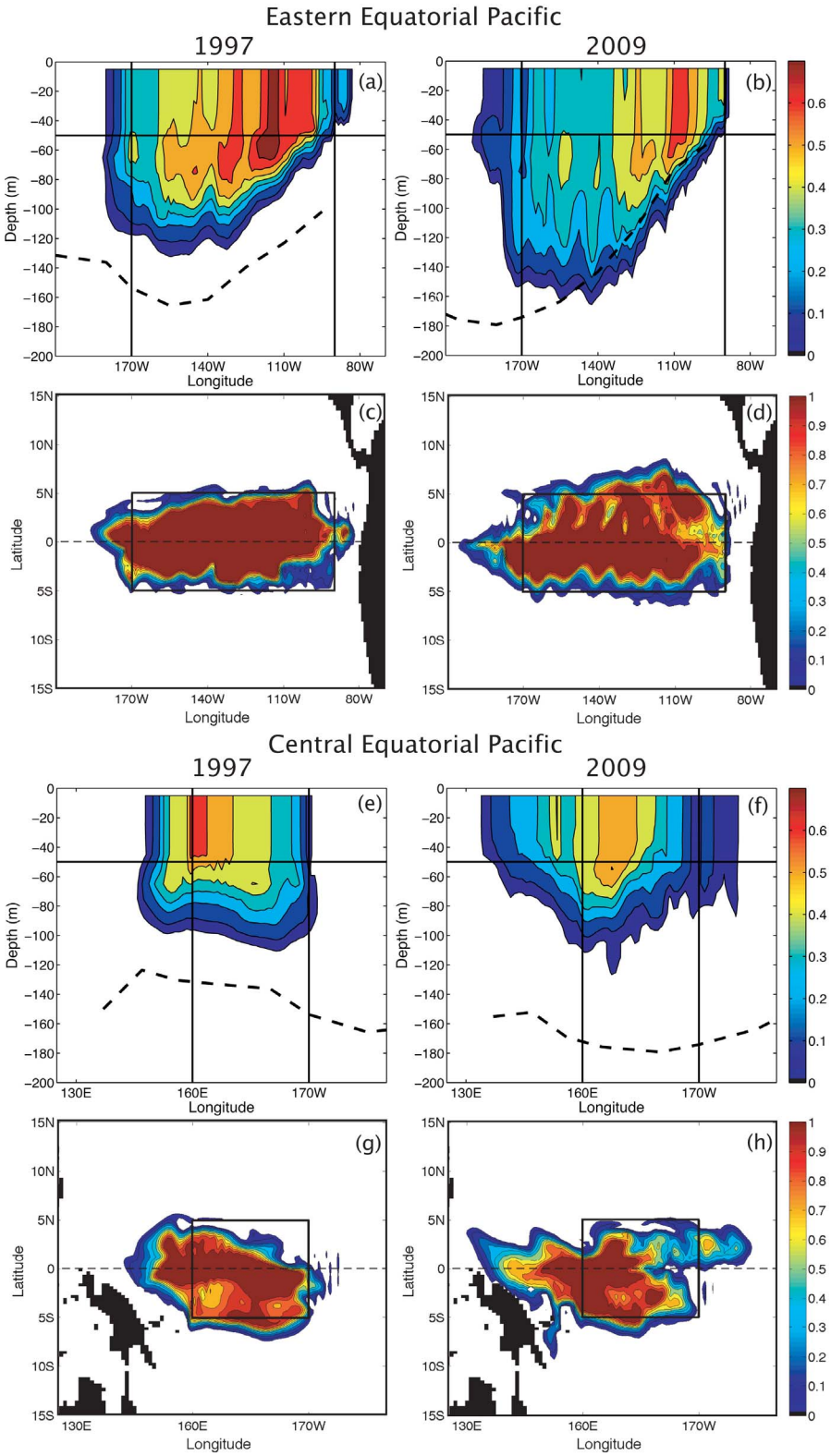

Figure 3. Normalized adjoint tracer concentrations in October 1997 and October 2009, initialized in the (a–d) EEP (5°S–5°N, 170°W–90°W) and (e–h) CEP (5°S–5°N, 160°E–170°W) in December. Figures 3a, 3b, 3e, and 3f illustrate the longitude-depth distribution of adjoint tracer values integrated from 5°S–5°N, and Figures 3c, 3d, 3g, and 3h illustrate the horizontal distribution of tracer concentrations integrated from 0–160 m. The dashed black lines in Figures 3a, 3b, 3e, and 3f denote the 20°C isotherm depth (5°S–5°N average) from the TAO buoy array. The 20°C isotherm depth is a proxy for the thermocline/nutricline.

to as C(x,z). For October 1997 and 2009, the C(x,z) fields showed that December waters in the upper 50 m of the EEP primarily came from a similar longitude range with substantial contribution from below 50 m, reflecting the roles of vertical advection (upwelling) and mixing. The occurrence of tracer distribution values below 50 m (i.e., the initialization depth) indicates that vertical mixing and advection did not completely vanish during the October-December time frame as a whole for either El Niño, but vertical processes were more reduced in 1997 compared to 2009 (as denoted by the differences in tracer depth). There was also secondary contribution of waters from the west by anomalous eastward surface currents that develop during El Niño as shown by the westward extension of tracer distributions from the EEP region (Figures 3a–3d). The major difference between these two patterns was that December waters in the upper 50 m of the EEP came from greater depths that extended to the thermocline/nutricline in 2009 (∼165 m) than in 1997 (∼135 m) (Figures 3a and 3b). This deeper source of upwelled water in 2009 introduced waters with higher nutrient concentrations into the upper EEP, consistent with a less notable chl-a reduction in the EEP during the 2009–10 CP-El Niño when compared with the 1997–98 EP-El Niño.

[11] Figures 3c and 3d illustrate the horizontal distribution of tracer concentrations integrated from 0 to 160 m, C(x,y) (normalized by the maximum initial tracer concentration integrated over the same depth). One major difference was that the 2009 event was more influenced by water north of 5°N, which reflects the role of horizontal and vertical mixing associated with tropical instability waves (TIWs) that did not completely vanish during the 2009–10 El Niño (in contrast to the 1997–98 El Niño). The TIW pattern was evident in the C(x,y) field for October 2009. The 2009 TIWs brought lower nutrient waters from north of 5°N into the EEP and reduced chl-a. This effect was overwhelmed by the larger nutrient supply from vertical advection and mixing in the EEP (compared to the 1997 event) since the chl-a reduction during the 2009–10 CP-El Niño was not as large as the 1997–98 EP-El Niño.

[12] Figures 3e–3h show the C(x,z) and C(x,y) fields in October 1997 and 2009 initialized from the CEP region. The major difference between the two events was that more western-Pacific warm-pool waters intruded into the CEP in 2009 than in 1997, especially in the surface layer. This pattern is consistent with surface current anomalies shown in Figure 1. Waters within the CEP and those intruding from the WEP were nutrient-poor as indicated by the depth of the thermocline/nutricline (Figures 3e and 3f). There was also a small contribution of waters from the east in 2009 (as seen from the small values of tracer concentration) that was due to advection and mixing associated with TIWs, which were not observed in 1997 (Figures 3g and 3h). The larger eastward intrusion of nutrient-depleted warm-pool water into the CEP explained the larger chl-a reduction during the 2009–10 CP-El Niño when compared to the 1997–98 EP-El Niño.

[13] In summary, the major differences in adjoint tracer distribution between the 1997–98 EP- and 2009–10 CP-El Niño indicated that (1) reduced chl-a in the EEP in 1997 was due to weaker trade winds that substantially reduced upwelling and vertical mixing to inhibit the supply of nutrients to the surface layer of the EEP, and (2) reduced chl-a in the CEP in 2009 was associated with stronger westerly wind anomalies in the WEP and CEP that caused a larger anomaly of eastward surface currents, which advected nutrient-depleted warm-pool waters into the CEP. The physical processes that controlled the chl-a response in the EEP and CEP parallel the processes that control SST on ENSO time scales, specifically the more dominant role of vertical/subsurface processes (horizontal advection) in the EEP (CEP) [e.g., *Wang and McPhaden*, 2000; *An and Jin*, 2001].

4. Concluding Remarks

[14] Satellite data and adjoint passive tracer simulations based on an ECCO ocean reanalysis product were used to characterize the difference in spatial structure of biological responses in the equatorial Pacific Ocean to the 1997–98 EP- and 2009–10 CP-El Niño and to explain the responsible mechanisms. Reduced chl-a was observed in the EEP (5°S–5°N, 170°W–90°W) and CEP (5°S–5°N, 160°E–170°W) during the 1997–98 EP-El Niño, and confined to the CEP during the 2009–10 CP-El Niño. The 1997–98 EP-El Niño event had a larger impact on chl-a in the EEP and the 2009–10 CP-El Niño a larger impact on chl-a in the CEP. Such biological responses were dependent on the strength and extent of westerly wind anomalies and their impact on the physical environment. Horizontal advection was the primary contributor to differences in chl-a between the two El Niño events in the CEP, whereas vertical advection and mixing processes in chl-a was observed in the EEP during the 1997–98 EP-El Niño than during the 2009–10 CP-El Niño as a result of weaker easterly trade winds that prompted less upwelling and vertical mixing. Within the CEP, chl-a was more reduced during the 2009–10 CP-El Niño compared to the 1997–98 EP-El Niño because of stronger eastward advection of nutrient-depleted waters from the WEP in association with westerly wind anomalies and eastward surface currents.

[15] This study implies that systematic changes in ENSO characteristics, as have been shown in recent studies of EP- and CP-El Niño events over the past three decades, could cause systematic differences in biological production through modification of the physical state of the ocean. If such a low-frequency trend continues then the CEP may experience lower biological productivity and the EEP slightly higher productivity on decadal time scales, which translates to possible restructuring of the marine ecosystem (i.e., regime shifts and species succession) and alteration of the equatorial Pacific carbon cycle. Such a systematic change in biological production has important socioeconomic implications for fishery industries in open ocean and coastal regions. The assessment of decadal change in biological production in response to ENSO diversity is limited by the relatively short duration of continuous ocean color satellite measurements (i.e., 1997-present), but will become possible with continuation in present and future missions. With improved understanding of the differences in the biological and physical state of the ocean to ENSO diversity, the response to future events can be better predicted and thereby improved management strategies can be instituted for coastal and open ocean environments.

[16] **Acknowledgments.** The research described in this paper was carried out at the Jet Propulsion Laboratory, California Institute of Technology, under a contract with NASA. The authors would like to thank Peter Strutton and the reviewers for all their helpful comments and suggestions. MJM was

supported by NOAA. PMEL contribution 3789. LDEO contribution 7542 and partial support from CERC in Ocean and Technology, Canada.

[17] The Editor thanks two anonymous reviewers for assisting with the evaluation of this paper.

References

An, S. I., and F.-F. Jin (2001), Collective role of thermocline and zonal advective feedbacks in the ENSO mode, *J. Clim.*, *14*, 3421–3432, doi:10.1175/1520-0442(2001)014<3421:CROTAZ>2.0.CO;2.

Ashok, K., and T. Yamagata (2009), Climate change: The El Niño with a difference, *Nature*, *461*, 481–484, doi:10.1038/461481a.

Ashok, K., S. K. Behera, S. A. Rao, H. Weng, and T. Yamagata (2007), El Niño Modoki and its possible teleconnection, *J. Geophys. Res.*, *112*, C11007, doi:10.1029/2006JC003798.

Atlas, R., R. N. Hoffman, J. Ardizzone, S. M. Leidner, J. C. Jusem, D. K. Smith, and D. Gombos (2011), A cross-calibrated, multiplatform ocean surface wind velocity product for meteorological and oceanographic applications, *Bull. Am. Meteorol. Soc.*, *92*, 157–174, doi:10.1175/2010BAMS2946.1.

Barber, R. T., and F. P. Chavez (1983), Biological consequences of El Niño, *Science*, *222*, 1203–1210, doi:10.1126/science.222.4629.1203.

Bonjean, F., and G. S. E. Lagerloef (2002), Diagnostic model and analysis of the surface currents in the tropical Pacific Ocean, *J. Phys. Oceanogr.*, *32*, 2938–2954, doi:10.1175/1520-0485(2002)032<2938:DMAAOT>2.0.CO;2.

Chavez, F. P., P. G. Strutton, and M. J. McPhaden (1998), Biological-physical coupling in the central equatorial Pacific during the onset of the 1997–98 El Niño, *Geophys. Res. Lett.*, *25*, 3543–3546, doi:10.1029/98GL02729.

Chavez, F. P., P. G. Strutton, G. E. Friederich, R. A. Feely, G. C. Feldman, D. G. Foley, and M. J. McPhaden (1999), Biological and chemical response of the equatorial Pacific Ocean to the 1997–98 El Niño, *Science*, *286*, 2126–2131, doi:10.1126/science.286.5447.2126.

Fiedler, P. C., F. P. Chavez, D. W. Behringer, and S. B. Reilly (1992), Physical and biological effects of Los Niños in the eastern tropical Pacific, 1986–1989, *Deep Sea Res., Part A*, *39*, 199–219, doi:10.1016/0198-0149(92)90105-3.

Fukumori, I., T. Lee, B. Cheng, and D. Menemenlis (2004), The origin, pathway, and destination of Niño-3 water estimated by a simulated passive tracer and its adjoint, *J. Phys. Oceanogr.*, *34*, 582–604, doi:10.1175/2515.1.

Kao, H.-Y., and J.-Y. Yu (2009), Contrasting eastern-Pacific and central-Pacific types of ENSO, *J. Clim.*, *22*, 615–632, doi:10.1175/2008JCLI2309.1.

Kim, H.-M., P. J. Webster, and J. A. Curry (2009), Impact of shifting patterns of Pacific Ocean warming on North Atlantic tropical cyclones, *Science*, *325*, 77–80, doi:10.1126/science.1174062.

Kim, S.-B., T. Lee, and I. Fukumori (2007), Mechanisms controlling the interannual variation of mixed layer temperature averaged over the Niño-3 region, *J. Clim.*, *20*, 3822–3843, doi:10.1175/JCLI4206.1.

Kug, J.-S., F.-F. Jin, and S.-I. An (2009), Two types of El Niño events: Cold tongue El Niño and warm pool El Niño, *J. Clim.*, *22*, 1499–1515, doi:10.1175/2008JCLI2624.1.

Larkin, N. K., and D. E. Harrison (2005), Global seasonal temperature and precipitation anomalies during El Niño autumn and winter, *Geophys. Res. Lett.*, *32*, L16705, doi:10.1029/2005GL022860.

Latif, M., R. Kleeman, and C. Eckert (1997), Greenhouse warming, decadal variability, or El Niño? An attempt to understand the anomalous 1990s, *J. Clim.*, *10*, 2221–2239, doi:10.1175/1520-0442(1997)010<2221:GWDVOE>2.0.CO;2.

Lee, T., and M. J. McPhaden (2010), Increasing intensity of El Niño in the central-equatorial Pacific, *Geophys. Res. Lett.*, *37*, L14603, doi:10.1029/2010GL044007.

Lee, T., I. Fukumori, D. Menemenlis, Z. Xing, and L.-L. Fu (2002), Effects of the Indonesian Throughflow on the Pacific and Indian Oceans, *J. Phys. Oceanogr.*, *32*, 1404–1429, doi:10.1175/1520-0485(2002)032<1404:EOTITO>2.0.CO;2.

McPhaden, M. J., S. E. Zebiak, and M. H. Glantz (2006), ENSO as an integrating concept in Earth science, *Science*, *314*, 1740–1745, doi:10.1126/science.1132588.

McPhaden, M. J., T. Lee, and D. McClurg (2011), El Niño and its relationship to changing background conditions in the tropical Pacific Ocean, *Geophys. Res. Lett.*, *38*, L15709, doi:10.1029/2011GL048275.

Radenac, M.-H., F. Léger, A. Singh, and T. Delcroix (2012), Sea surface chlorophyll signature in the tropical Pacific during eastern and central Pacific ENSO events, *J. Geophys. Res.*, *117*, C04007, doi:10.1029/2011JC007841.

Reynolds, R. W., T. M. Smith, C. Liu, D. B. Chelton, K. S. Casey, and M. G. Schlax (2007), Daily high-resolution-blended analyses for sea surface temperature, *J. Clim.*, *20*, 5473–5496, doi:10.1175/2007JCLI1824.1.

Strutton, P. G., and F. P. Chavez (2000), Primary productivity in the equatorial Pacific during the 1997–1998 El Niño, *J. Geophys. Res.*, *105*, 26,089–26,101, doi:10.1029/1999JC000056.

Turk, D., M. R. Lewis, G. W. Harrison, T. Kawano, and I. Asanuma (2001), Geographical distribution of new production in the western/central equatorial Pacific during El Niño and non-El Niño conditions, *J. Geophys. Res.*, *106*, 4501–4515, doi:10.1029/1999JC000058.

Turk, D., C. S. Meinen, D. Antoine, M. J. McPhaden, and M. R. Lewis (2011), Implications of changing El Niño patterns for biological dynamics in the equatorial Pacific Ocean, *Geophys. Res. Lett.*, *38*, L23603, doi:10.1029/2011GL049674.

Wang, O., I. Fukumori, T. Lee, and B. Cheng (2004), On the cause of eastern equatorial Pacific Ocean T-S variations associated with El Niño, *Geophys. Res. Lett.*, *31*, L15309, doi:10.1029/2004GL020188.

Wang, W., and M. J. McPhaden (2000), The surface layer heat balance in the equatorial Pacific Ocean. Part II: Interannual variability, *J. Phys. Oceanogr.*, *30*, 2989–3008, doi:10.1175/1520-0485(2001)031<2989:TSLHBI>2.0.CO;2.

Weng, H., S. K. Behera, and T. Yamagata (2009), Anomalous winter climate conditions in the Pacific rim during recent El Niño Modoki and El Niño events, *Clim. Dyn.*, *32*, 663–674, doi:10.1007/s00382-008-0394-6.

Yu, J.-Y., and H.-Y. Kao (2007), Decadal changes of ENSO persistence barrier in SST and ocean heat content indices: 1958–2001, *J. Geophys. Res.*, *112*, D13106, doi:10.1029/2006JD007654.

Yu, J.-Y., and S. T. Kim (2010), Three evolution patterns of central-Pacific El Niño, *Geophys. Res. Lett.*, *37*, L08706, doi:10.1029/2010GL042810.